ACS APPLIED MATERIALS & INTERFACES

RESEARCH ARTICLE

www.acsami.org

Electron and Phonon Transport in Au Nanoparticle Decorated Graphene Nanoplatelet Nanostructured Paper

Jinglei Xiang and Lawrence T. Drzal*

Department of Chemical Engineering and Materials Science, Michigan State University, East Lansing, Michigan 48824-1226, United States

Supporting Information

ABSTRACT: Monodispersed Au nanoparticles are synthesized on the surface of exfoliated graphene nanoplatelets (GNP) in the presence of polyethyleneimine (PEI) with microwave assisted heating. A highly structured layered Au/GNP "paper" with good flexibility and mechanical robustness is prepared by vacuum assisted self-assembly. The thermal and electrical conductivity of the hybrid paper with and without the Au nanoparticles are investigated after different experimental processing conditions including thermal annealing and cold compaction. Annealing effectively decomposes and removes the adsorbed PEI molecules and improves thermal contact between Au/GNP particles, whereas cold compaction reduces porosity and induces stronger alignment of the Au/GNP within the hybrid paper. Both approaches lead to improvement in electrical and thermal conductivity. It is also found that adjacent GNP particles are electrically connected by the Au nanoparticles but thermally disconnected. It is believed that phonons are scattered at the Au/GNP interfaces, whereas electrons can tunnel across this interface, resulting in a separation of electron and phonon transport within this hybrid paper.

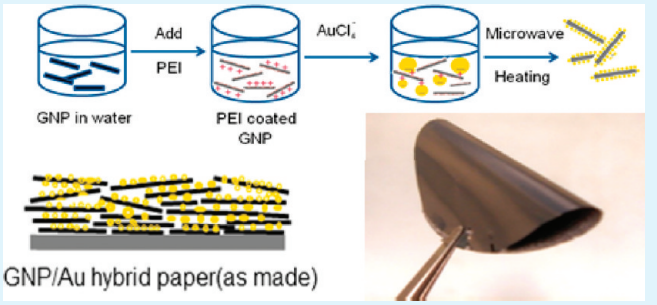

KEYWORDS: graphene nanoplatelets, polyethyleneimine, Au/graphene nanoplatelet hybrid, annealing, cold compaction

INTRODUCTION

Numerous research efforts are underway directed at discovering the superior and unique properties of single layer graphene and multilayer graphene nanoplatelets.[1−4] In particular, graphene-metal nanoparticle hybrid systems have the potential to be very useful in various engineering applications such as fuel cell catalysis,[5−9] electrochemical sensing[10,11] and electrochemical energy storage.[12,13] Several methods to synthesize metal nanoparticles on the basal plane surface of graphene have been explored quite extensively. Among those, solution and supercritical liquid approaches have the advantage of covering the entire surface area of graphene nanoplatelets. For example, one common method to synthesize metal nanoparticles is to chemically functionalize the graphitic surface in order to induce anchoring sites for the metal precursors. The metal precursor is then reduced in the presence of a reducing agent to produce nanoparticles that covalently attaches to the basal plane of the graphene.[14−16] The downside of this approach is the disruption of the sp^2 bonded carbon atoms in the basal plane which leads to reduced transport properties of graphene because of additional scattering sites.[17] Another widely adopted technique involves noncovalent encapsulation of the graphitic surface with a surfactant or a polymer and subsequent growth of nanoparticles on the surfactant in the presence of a reducing agent.[18,19] This technique induces minimum chemical perturbation of the basal planes, preserving the conjugated system for undisrupted carrier transport. Other techniques of metal nanoparticle decoration on graphitic nanostructure include electro-deposition,[20] evaporation,[21] and solventless bulk synthesis.[22] Although these methods have some processing advantages over solution-phase techniques, they are usually quite expensive and energy intensive. To synthesize nanoparticles using the solution-phase approach with a narrow size distribution, several factors need to be controlled carefully, which include the concentration of metal salt and reducing agent,[23,24] the presence of a protecting agent,[25] the reaction time,[26] and reaction temperature.[27]

Despite the many publications on superior electrochemical properties of nanoparticle/graphene hybrids, none discuss the transport properties of this hybrid metal/graphene nanoplatelet material when made into a paperlike structure where the nanoparticles are located at the surfaces and interfaces of the graphene nanoplatelets.

In this work, we synthesized monodispersed gold nanoparticles on exfoliated graphene nanoplatelets (GNP) in the presence of a polyethyleneimine matrix with microwave assisted heating.[28] Previous publications have reported on the deposition of Au nanoparticles on graphene nanosheets through simultaneous reduction of graphene oxide and Au(III) by microwave heating and sonolysis.[29,30] This work demonstrates a fast, one-pot,

Received: January 29, 2011
Accepted: March 15, 2011
Published: March 25, 2011

Scheme 1. Schematics of Experimental Procedures and the Interactions between the Metal Ions and the Active Sites on PEI Coated GNP and Formation of Au Nanoparticles

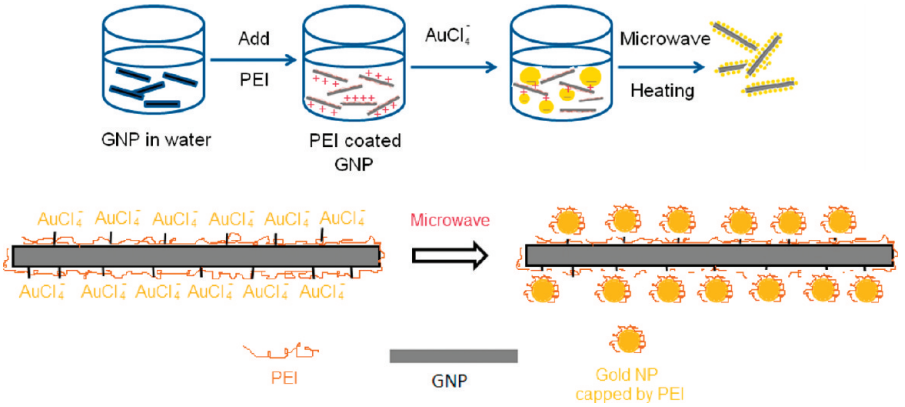

aqueous synthesis of Au nanoparticles directly on pristine graphene nanosheets. GNPs are few layer graphene nanosheets produced from microwave exfoliation of graphite intercalated compounds followed by a combination of size reduction processes. Research conducted in MSU has led to a process that can successfully produce exfoliated graphene nanoplatelets with controlled thicknesses ranging from 1 to 10 nm and platelet diameters from 100 to 10000 nm.[31,32] Polyethyleneimine, a hydrophilic polymer with primary, secondary and tertiary amino groups and an overall positive charge in the neutral aqueous solution, adsorbs on the highly hydrophobic GNP surface and stabilizes the GNP particles in water. The adsorption of PEI on GNP effectively induces both electrostatic and steric stabilization.[33] In addition, PEI contains one of the highest densities of amino groups among all polymers, donating electrons that help reduce metal ions.[34−36] Gold nanoparticles were chosen here because of their strong resistance to oxidation and excellent thermal and electrical properties. Gold nanoparticle decorated GNP was prepared into a thin multilayered "paper" by vacuum assisted self-assembly. The electrical and thermal conductivity of the Au/GNP paper was characterized. It is believed that the presence of PEI that either encapsulates the Au nanoparticles or adsorbs on the GNP particle is likely to interfere with both electron and phonon transport within the hybrid paper. Therefore, a thermal annealing treatment was applied to remove the PEI within the paper by thermal decomposition. Since the GNP is highly oxidation resistant to temperatures greater than 500 °C, chemical changes in the GNP did not take place during annealing. It is also worth noting that the hybrid paper sample as prepared by self-assembly is highly porous, which would affect the electrical and thermal conductivities of the paper significantly. To reduce porosity and enhance particle alignment in the paper, the annealed samples were compacted in a hydraulic press at room temperature. The impact of gold nanoparticles on both electron and phonon transport in this hybrid paper under different experimental conditions (thermal annealing, cold compaction) is discussed.

RESULTS AND DISCUSSION

Dispersion of GNP particles in water proves difficult and results in an immediate floating and aggregation of the particles at the air−water interface because of the highly hydrophobic nature of the basal plane. Polyethyleneimine, a cationic polyelectrolyte, adsorbs on the GNP surface due to a thermodynamic driving force to reduce the hydrophobic-hydrophilic interfacial area between GNP and water to minimize the interfacial energy.[18] At pH <10, the positively charged polymer chain also induces electrostatic repulsion that contributes to good dispersion of the nanoplatelets. As the tetrachloroauric acid dissolved in water was mixed with the GNP suspensions, the $AuCl_4^-$ ions complex with the positive functional groups of PEI adsorbed on the GNP surface (chloride ligands were replaced by amine groups of PEI). The adsorbed PEI chains, in this case, serve as templates for subsequent Au nanoparticle growth on the surface of GNP. The addition of H^+ ions also lowers the pH of the solution to around 6, inducing more positive charges on the chain of PEI and more electrostatic attraction with $AuCl_4^-$.[37] The reduction of Au^{3+} to Au^0 was then carried out in a microwave oven where the heating rate is fast enough to cause a rapid temperature increase in the solution due to the high polarity of water molecules, creating a high concentration of radicals that facilitates the electron transfer from the radicals of PEI to the metal precursor. As soon as the solution is supersaturated with metal atoms, Au atoms form nuclei. The critical size of the nucleus as well as nucleation activation energy control the nucleation rate and depend on the surface tension of the nuclei−solvent interface when the radius of nuclei is small.[38,39] Therefore, a higher surface tension corresponds to a larger critical nucleus size and a lower nucleation rate, which should be avoided in synthesizing monodispersed small nanoparticles. Upon formation of the nucleus, polyethyleneimine, with a lower surface tension than Au atoms, adsorbs on the surface of the metal atoms reducing the nucleation energy barrier and critical nucleus size. As a result, more primary particles with low surface energy are formed leading to generation of smaller secondary particles whose growth and coarsening are also affected by surface tension.[40] In addition, the low interfacial energy of PEI also contributes to the stabilization of the Au nanoparticles in the solution. Scheme 1 represents the typical procedures and the interactions between the metal ions and the active sites on GNP particles and subsequent formation of nanoparticles on GNP.

From scanning electron micrographs shown in Figure 1, it is found that the size and loading of the Au nanoparticles synthesized by this technique correlated with the concentration of PEI in the solution. The size of the nanoparticles was reduced while the loading increased with higher concentration of PEI in the

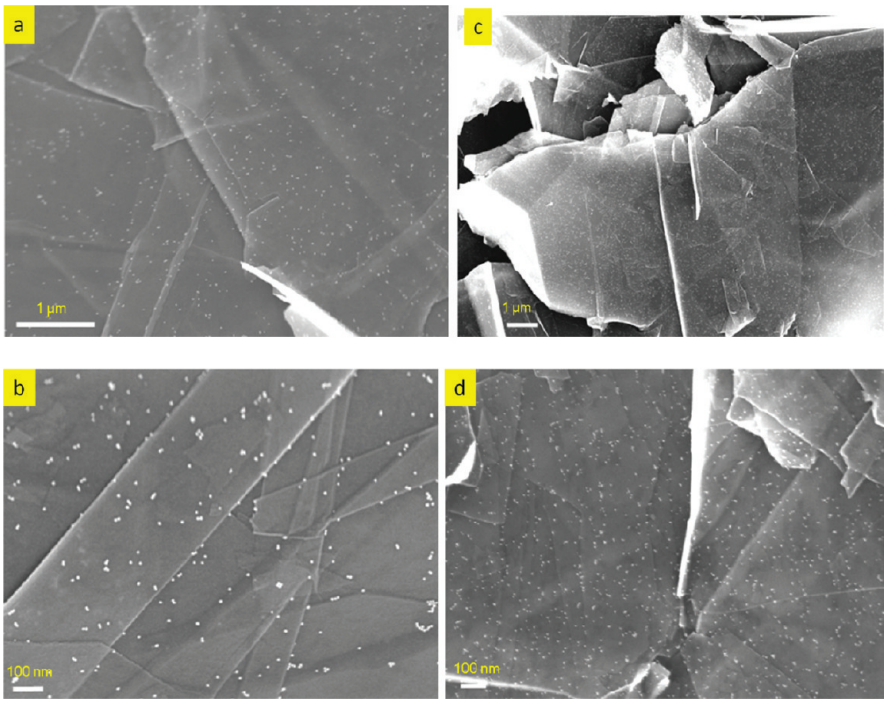

Figure 1. (a, b) Low- and high-magnification SEM images of Au nanoparticle decorated GNP prepared at 0.3 wt % PEI concentration. (c, d) Low- and high-magnification SEM images of Au nanoparticle decorated GNP prepared at 0.6 wt % PEI concentration.

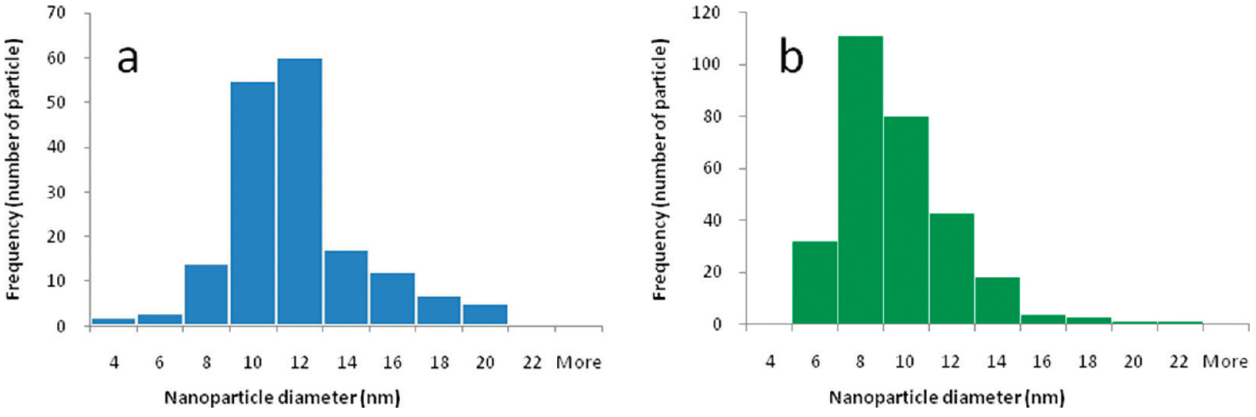

Figure 2. (a) Size and distribution of Au nanoparticles on GNP prepared at 0.3 wt % PEI concentration. (b) Size and distribution of Au nanoparticles on GNP prepared at 0.6 wt % PEI concentration.

solution. With a higher concentration of PEI in the solution, the number of nuclei with a lower surface energy increased which leads to formation of more primary and secondary particles. In addition, more PEI chains would adsorb on to the surface of GNP acting as templates for Au nanoparticle growth. There is no obvious agglomeration of Au nanoparticles on the surface of GNP, which is also believed to be the result of PEI encapsulation that stabilizes the nanoparticles in the solution electrostatically. Figure 2 shows the size and distribution of Au nanoparticles on the GNP surface at 0.3 and 0.6 wt % PEI concentrations. This is obtained by analyzing representative SEM images of magnifications at 80k or higher in Image-Pro, a commercially available software (see the Supporting Information). It is clear that the whole spectrum shifts to a smaller size range while the number of nanoparticles increased for samples prepared in 0.6 wt % PEI. The size of the Au nanoparticles prepared at 0.3 wt % PEI is 10.8 ± 2.4 nm, whereas they are reduced in size to 8.3 ± 2.1 nm at 0.6 wt % PEI.

Scheme 2 shows the vacuum-assisted self-assembly process to prepare Au/GNP hybrid paper. To create a more ordered multilayer structure within the paper, it is important to do multifiltration (5 mL at a time) instead of filtration all at once. After the filtration process, it is found that the bottom few layers in contact with the filter membrane is more ordered than the top layers as a result of a nonuniform pressure difference in the paper during filtration as thickness builds up. Therefore, $30 - 40$ mL of Au/GNP suspension at 1 mg/mL concentration was filtered to achieve a better aligned structure within the hybrid paper. Figure 3 shows the photos of the as-made papers after being removed from the filter membrane. The as-made paper is very flexible and shows certain mechanical robustness under bending.

The cross sections of both as-made GNP and Au/GNP papers for SEM observation were prepared by epoxy embedding shown in Figure 4. The neat as-made GNP paper shows a highly aligned structure while preserving certain porosity introduced during filtration. However, porosity is higher in the Au/GNP hybrid paper. The observed difference in morphology is attributed to the presence of Au nanoparticles on GNP. The Au nanoparticles act as spacers, creating more gaps between individual nanoplatelets when they are assembled into a paper. Due to the more open structure of the hybrid "paper", epoxy can easily penetrate into the gaps as shown in Figure 4b. However, a highly ordered and highly condensed structure was formed after annealing and cold compaction. The increase in porosity for Au/GNP hybrid sample can also be supported by a reduction in the apparent density of the paper which is shown in Table 1.

Thermal diffusivity of the samples prepared at different experimental conditions (as-made, annealed, annealed and cold compacted) were measured. Given the density of the sample, and the specific heat, which was measured by differential scanning calorimetry, thermal conductivity of the sample can be obtained: $\kappa = \alpha\rho C_p$, where κ is thermal conductivity with a unit of W/(m K), α is thermal diffusivity with a unit of mm^2/s, and C_p is specific heat with a unit of J/(g K).

As shown in Figure 5a, the through-plane thermal diffusivity of all the samples followed the same trend with a slight increase after thermal annealing and a reduction after cold compaction. Previous work showed that the enhancement brought by annealing was due to the thermal decomposition of polyethyleneimine at 300 °C[41] (see the Supporting Information). It is believed PEI adsorbed either on the GNP surface or on the Au nanoparticles scatter the phonons in this paperlike structure, contributing to a larger thermal interface resistance which is a major impediment to phonon transport.[42,43] A thermal annealing treatment removed most of the PEI in the paper, presumably reducing the interfacial resistance as suggested by a 20% improvement in through-plane diffusivity. However, upon annealing and cold compaction, thermal diffusivity decreased for all the samples. Compaction of the sample effectively eliminated large pores within the paper created during filtration and the nanoplatelets were more aligned due to the compressive stress. The better orientation of the nanoplatelets reduced the through-plane phonon transport due to the intrinsically low thermal conductivity of GNP with multiple layers of graphene held together with weak van der Waals forces and the high probability of interface scattering between individual nanoplatelets. It is also found that the through-plane diffusivity of the Au/GNP hybrid paper is lower than the neat GNP paper. The existence of Au nanoparticles on GNP is likely to interfere with GNP from making contact with each other and the paper becomes more porous. As a result, thermal diffusivities for the as-made samples reduce with an increasing concentration of Au nanoparticles on the GNP surfaces.

Cold compaction will densify the "loose" porous nanostructure. Despite the fact that macro sized pores collapse upon compaction in neat GNP paper, there are still numerous slit pores inside it that would interfere with the transport of electrons and phonons. With the hybrid paper, Au nanoparticles on the surface of GNP now have a much higher probability of contact with each other, serving as bridging agents or mini columns which might facilitate propagation of phonons within the paper structure. Nonetheless, the experimental results for "annealed and cold compacted" samples indicated a reduction in the through-plane diffusivity for the Au/GNP hybrid paper. In this case, a phonon is forced to go through a Au nanoparticle to go from one GNP to another, which slows down the heat transfer, thus the thermal diffusivity. The same trend can be observed for thermal conductivity of the samples. In particular, the cross sectional area of heat conduction is reduced due to the presence of Au nanoparticles. As a result, the through-plane thermal conductivity of the Au/GNP hybrid sample is lower than the neat GNP paper after annealing and cold compaction. The result is shown in Figure 5b. As a comparison, the reported through-plane thermal conductivity for the highly oriented pyrolytic graphite measured by pump−probe thermoreflectance technique is 6.1 W/(m K).[44]

The in-plane thermal diffusivity and conductivity are shown in Figure 5c-d. Thermal annealing causes decomposition and removal of PEI from within the sample, improving the "thermal contact area" by reducing interface resistance. A moderate increase of around 10% was observed for samples measured after annealing. Cold-compaction of the samples restores the orientation of the nanoplatelets, making the paper more anisotropic in

Scheme 2. Schematics of the Experiment Showing the Au Nanoparticle Decorated GNP Dispersed in Water for Subsequent Vacuum-Assisted Self Assembly

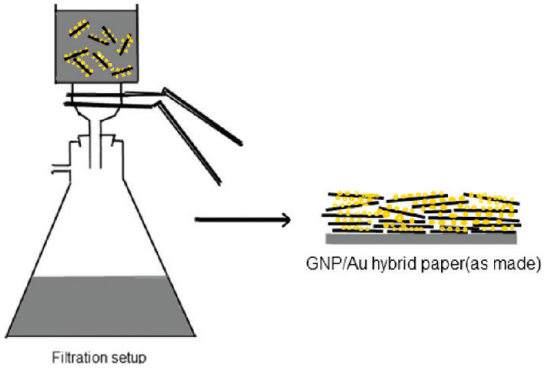

Figure 3. Photos of the as-made GNP paper showing flexibility and mechanical robustness under bending and the Au/GNP hybrid sample used for thermal diffusivity measurement (1 in. diameter).

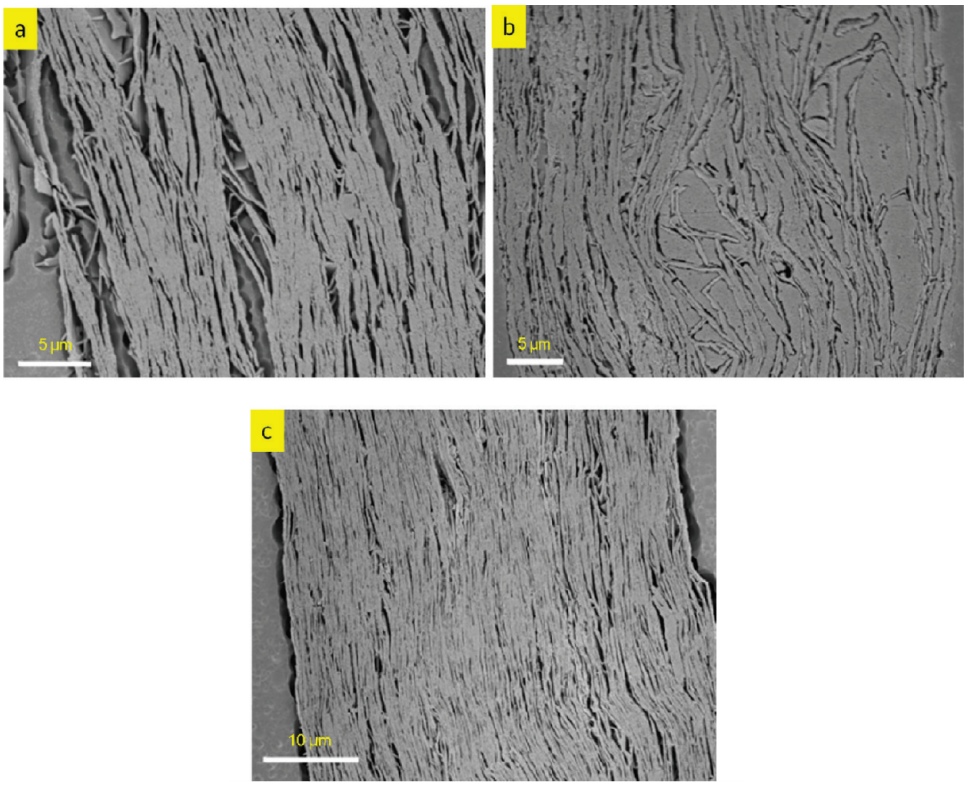

Figure 4. (a) Representative cross-sectional SEM image of "as-made" GNP paper. (b) As-made Au/GNP hybrid paper (0.3 wt % PEI). (c) "Annealed and cold compacted" GNP paper.

Table 1. Average Densities of GNP and Au/GNP Hybrid Papers Measured As-Made, Annealed, Annealed & Cold Compacted (standard deviation <0.05 g/cm^3)

	density, ρ (g/cm^3)		
	as-made	annealed	annealed & cold compacted
GNP paper	0.62	0.62	1.5
Au/GNP (0.3 wt % PEI)	0.58	0.57	1.5
Au/GNP (0.6 wt % PEI)	0.58	0.58	1.5

heat conduction. In particular, the thermal conductivity of all "annealed and cold compacted" samples improve by almost 70% with neat GNP paper approaching as high as 200 W/(m K). It is worth noting that both thermal diffusivity and conductivity of the Au/GNP hybrid samples are lower than the neat GNP paper, which is in accord with the trend observed from through-plane measurements. It is believed that those Au nanoparticles are more likely to serve as phonon scatterers than mini heat conduction channels within the hybrid samples. Recent work by Wang et al used a thermal bridge configuration to measure the in-plane thermal conductivity of supported few layer graphene nanosheets and concluded that the conductivity is 1250 W/(m K) at room temperature is comparable to bulk graphite.[45] The value reported here is lower because of the strong interface scattering which is absent in either individual graphene nanosheets or bulk graphite.

The self-assembly of GNP with and without Au nanoparticles did have an impact on the thermal conductivity of the samples. In particular, the gold nanoparticles that were expected to provide additional heat channels through the plane of the paper structure to improve the heat conduction turned out to be ineffective. To investigate if the same phenomenon observed in phonon transport also applies to electrons, both the through-plane and in-plane electrical conductivity of these papers were measured and reported in panels a and b in Figure 6.

From Figure 6a, the in-plane electrical conductivity of the papers increased with annealing and cold compaction. The improvement can be explained by the effective decomposition of electrically insulating PEI from the samples through thermal annealing and significant reduction of pore volumes through cold compaction, both contributing to decreasing electron tunneling resistance. In particular, the GNP paper decorated with Au nanoparticles of different size and distribution density showed higher conductivity than the neat GNP paper. Hybrid GNP papers with individual nanoplatelets decorated with smaller and higher coverage of Au nanoparticles exhibited higher in-plane electrical conductivity. Upon cold compaction, the collapse of macro pores in the sample brings more Au nanoparticles into immediate contact, effectively bridging previously isolated nanoplatelets. It is worth noting that the in-plane conductivity reaches a value as high as 1500 S/cm for Au/GNP (0.6 wt % PEI) hybrid paper, which is almost 70% higher than the neat GNP paper (880 S/cm) at the same condition. It is worth noting that the in-plane electrical conductivity is measured to be 2×10^4 S/cm for bulk graphite,[46] 1 order of magnitude higher than the value reported here for Au/GNP hybrid sample.

The through-plane electrical resistivity of the papers was measured by a two-point method (see the Supporting Information) on the samples that have been annealed and cold compacted. The result is shown in Figure 6b. The results from as-made and annealed samples are not reported because the

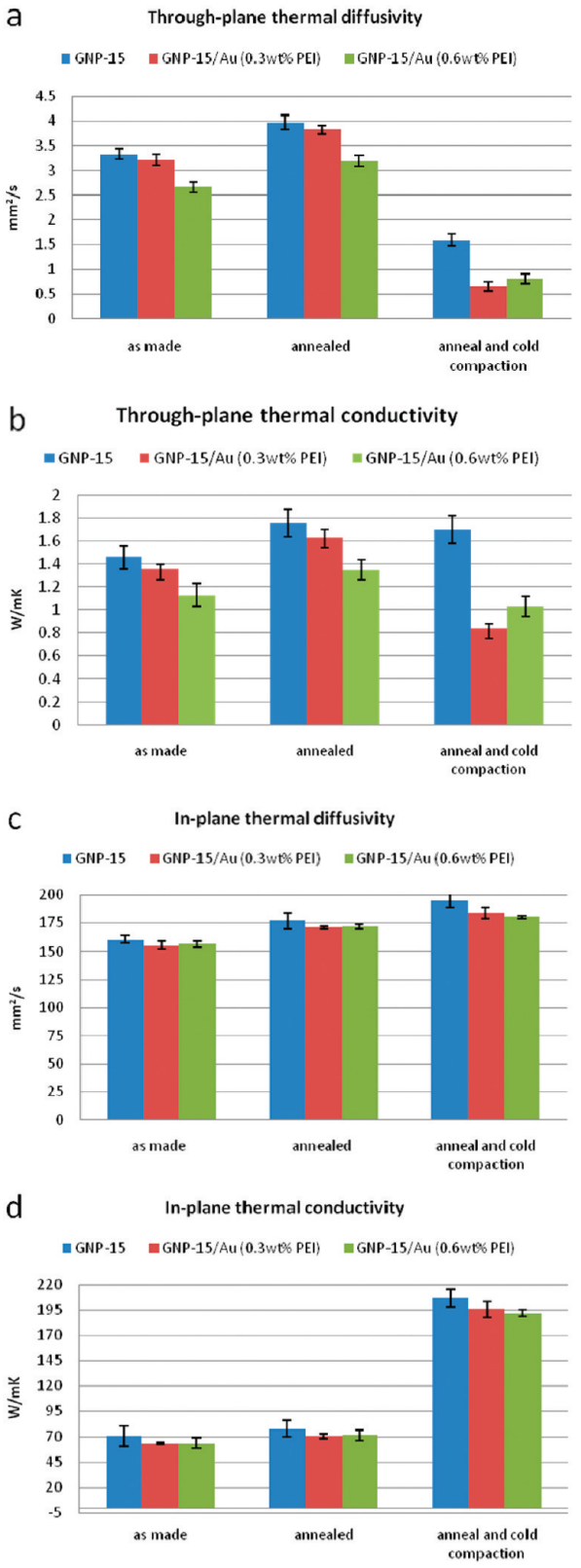

Figure 5. (a) Through-plane thermal diffusivity of GNP and Au/GNP paper. (b) Through-plane thermal conductivity of GNP and Au/GNP paper. (c) In-plane thermal diffusivity of GNP and Au/GNP paper. (d) In-plane thermal conductivity of GNP and Au/GNP paper.

measured electrical resistance fluctuates a large amount possibly due to the open porous structure inside the sample. The

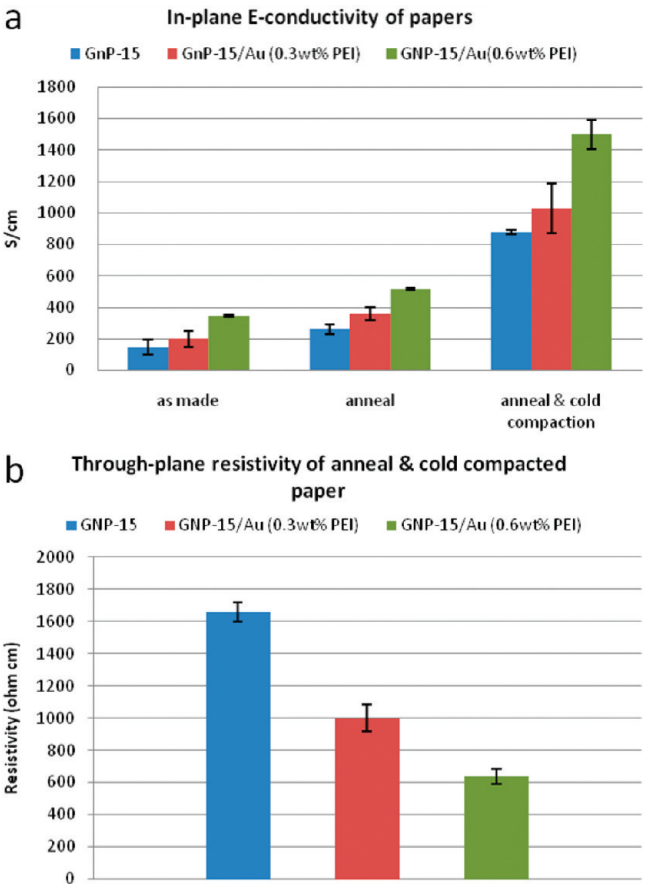

Figure 6. (a) Through-plane electrical resistivity of annealed and cold-compacted GNP and Au/GNP paper. (b) In-plane electrical conductivity of annealed and cold-compacted GNP and Au/GNP paper.

measurements on the annealed and cold compacted samples were stable enough thanks to the dense and compact structure of the paper. The Au nanoparticles effectively bridged adjacent GNPs, creating mini channels for the cross-plane electron transport as evidenced by the drop in the through-plane resistivity. It is thus evident that although the through-plane conductivity is small because of a greater anisotropic electronic conduction induced by cold compaction, the Au nanoparticles did facilitate the electron transport within the paper structure, making individual nanoplatelets more electrically connected. As a comparison, the through-plane resistivity for bulk graphite is 0.1−1 Ω cm, a few orders of magnitude lower than the highly ordered layer structure reported here.[46]

The findings reported here indicate that electron and phonon transport are affected differently by the presence of Au nanoparticles within the hybrid sample. Phonons travel at different frequencies in two materials of different densities (e.g., Au and graphite). Non-equilibrium molecular dynamic studies show that when a large mismatch in the phonon vibrational density of states (VDOS) exists in two distinctive mediums, direct coupling and propagation of phonons across the interface will be reduced. As a result, the thermal energy can only be transferred across the interface indirectly through anharmonic scattering which enables phonon−phonon interactions and gives rise to a high thermal interface resistance.[47] Despite the fact that Au nanoparticles could bridge the small gaps between individual nanoplatelets, the anharmonicity in VDOS in gold and carbon result in strong

interface scattering that reduces the efficiency of heat transfer. However, the improvement observed in electrical conductivity suggests that the Au nanoparticles allow more electrons to tunnel through, making the hybrid paper structure more electrically connected as compared with the neat GNP paper.

A few literature citations point out that few-layer graphene shows improved electrical conductivity when Au precursor were spontaneously reduced to Au nanoparticles driven by the redox potential difference between the Au^{3+} and the graphene nanosheets.[48−50] As a result, the few-layer graphene was p-type doped with electrons being transferred away from it to the metal precursor. The mere increase of the carrier concentration (i.e., holes) contributes to an increase in the electrical conductivity. However, the microwave assisted synthesis of nanoparticles in PEI matrix reported here did not involve transfer of electrons from individual graphite nanoplatelets to Au^{3+} ions. The fact that electrons mainly come from polyethyleneimine instead of GNP eliminates the possibility that the individual nanoplatelets would be p-type doped. Therefore, the enhancement in electrical conductivity observed here originates from the reduction in the interface resistance instead of doping, i.e., more electrons can find routes with least resistive pathways within the hybrid paper structure because of the highly electrically conductive Au nanoparticles.

CONCLUSION

Gold nanoparticles of a uniform size distribution were successfully synthesized on exfoliated graphene nanoplatelets by microwave assisted heating in a polyethyleneimine/water solution. It is believed that fast supersaturation of metal atoms with low surface tension is desired for producing monodispersed small nanoparticles. A self-standing, mechanically robust Au/GNP nanostructured multilayered "paper" was prepared by vacuum assisted self-assembly. Thermal annealing to decompose and remove PEI improves both electrical and thermal conductivities. Paper porosity was significantly reduced by cold compaction which produces closer contact between individual nanoplatelets. Au nanoparticles on the surface of GNP reduce phonon transport by introducing more scattering sites at the interface due to a vast difference in the vibrational density of states for phonons in gold and GNP and by reducing the total cross sectional area for heat conduction. However, the Au nanoparticles act as electron super highways that make nanoplatelets more electrically connected.

EXPERIMENTAL SECTION

Preparation of Exfoliated Graphene Nanoplatelets (GNP). GNPs were produced from a commercial graphite intercalated compound (Asbury Mills, NJ). Thermal exfoliation was carried out in a microwave oven followed by mechanical size reduction with a combination of ultrasonication and ball milling to produce nanoplatelets with the desired aspect ratios. GNP-15 refers to GNP particles with average diameters of about 15 μm with thickness less than 10 nm. GNP-15 particles are used throughout the experiment and are simply referred as GNP.

Decoration of GNP with Au Nanoparticles. Polyethyleneimine (PEI) was purchased from Sigma Aldrich (branched, M_w = 25 000). The GNP particles were dispersed in a PEI/water solution containing 0.3 wt % and 0.6 wt % PEI. The suspensions were bath sonicated for 1 h and kept stirred overnight to ensure sufficient interaction between PEI and GNP. Tetrachloroauric acid ($HAuCl_4 \cdot 3H_2O$) purchased from Sigma Aldrich (>99.9% trace metal basis) was then added into the suspension and mixed thoroughly. The suspension was irradiated with microwave radiation for a short period of time and then centrifuged at 6000 rpm and washed with copious amount of water to produce Au nanoparticle decorated GNP. The resulting Au/GNP product was dried under vacuum at 70 °C overnight.

Preparations of Au/GNP Hybrid Paper (As Made, Annealed, Annealed and Cold-Compacted). The Au/GNP hybrid paper was prepared by vacuum filtration with an ANODISC 47 mm filter membrane. (0.2 μm, Whatman) The hybrid paper was then washed with water and dried at 60 °C under vacuum overnight before being removed from the filter. These were identified as "as-made" samples. The paper identified as "annealed" sample was placed in a furnace and annealed at 340 °C in air for 2 h to decompose the PEI. The "annealed and cold compacted" paper was mechanically compressed in a hydraulic press at 100 psi at room temperature for 1 h. For comparison, a neat GNP paper without Au nanoparticles was prepared in the same way.

Flash Lamp Thermal Diffusivity Measurement by Nanoflash 447 (Netzsch Instruments). For through-plane thermal diffusivity measurement, the 1inch disk sample was placed in the sample holder covered by a ring shaped mask to block any leakage of light from sample edges. The entire bottom surface of the sample was irradiated and the heat propagating to the top surface was collected by the IR camera. The "cowan + pulse" model provided by the software package (Netzsch Proteous) was used to calculate thermal diffusivity. The in-plane diffusivity was measured using a method that employs a mask that collimates the laser beam at a 5 mm diameter spot at the bottom of the 1inch disk sample. Another mask with embedded annulus of 9 to 12 mm was placed on the sample allowing heat propagating radially to be collected. The "in-plane, anisotropic + heat loss" model incorporated in the software was used for subsequent diffusivity calculation.

Electrical Conductivity Characterizations of Hybrid Papers. In-plane electrical conductivity was measured with a Keithley 2400 SourceMeter in a four point configuration with a probe spacing of 1 cm on thin rectangular films. Electric current was scanned from 20 to 100 mA with 20 mA intervals. Voltage drops on the sample were recorded and plotted against the current to obtain the resistance. The through-plane conductivity of thin film samples was measured by using 2 instead of 4 leads. Electrical resistance of the sample was obtained by calculating the slope of the voltage vs current data. Taking the geometry of the samples into account, the in-plane electrical conductivity and through-plane resistivity were calculated.

ASSOCIATED CONTENT

Supporting Information. TGA curves showing thermal decomposition of PEI within the samples. Au nanoparticle size distribution analysis with Image-Pro and details of through-plane electrical resistivity measurement for thin films. This material is available free of charge via the Internet at http://pubs.acs.org.

AUTHOR INFORMATION

Corresponding Author
*Fax:+1 517 432 1634. E-mail: drzal@egr.msu.edu (L.T.D.).

ACKNOWLEDGMENT

The authors acknowledge the Army Research Office for financial support of this research, Grant W911NF-09-1-0451, Dr. Robert Mantz, Technical Program Manager.

REFERENCES

(1) Geim, A. K.; Novoselov, A. K. *Nat. Mater.* **2007**, *6*, 183–191.
(2) Avouris, P.; Chen, Z.; Perebeinos, V. *Nat. Nanotechnol.* **2007**, *2*, 605–615.
(3) Allen, M. J.; Tung, V. C.; Kaner, R. B. *Chem. Rev.* **2010**, *110*, 132–145.
(4) Rao, C. N. R.; Sood, A. K.; Subrahmanyam, K. S.; Govindaraj, A. *Angew. Chem., Int. Ed.* **2009**, *48*, 7752–7777.
(5) Xu, C.; Wang, X.; Zhu, J. *J. Phys. Chem. C.* **2008**, *112*, 19841–19845.
(6) Yoo, E.; Okata, T.; Akita, T.; Kohyama, M.; Nakamura, J.; Honma, I. *Nano Lett.* **2009**, *9*, 2255–2259.
(7) Li, Y. M.; Tang, L. H.; Li, J. H. *Electrochem. Commun.* **2009**, *11*, 846–849.
(8) Serger, B.; Kamat, P. V. *J. Phys. Chem. C.* **2009**, *113*, 7990–7995.
(9) Zhu, C.; Guo, S.; Zhai, Y.; Dong, S. *Langmuir.* **2010**, *26*, 7614–7618.
(10) Lu, J.; Do, I.; Drzal, L. T.; Worden, R. M.; Lee, I. *ACS Nano* **2008**, *2*, 1825–1832.
(11) Guo, S.; Wen, D.; Zhai, Y.; Dong, S.; Wang, E. *ACS Nano* **2010**, *4*, 3959–3968.
(12) Si, Y.; Samulski, E. *Chem. Mater.* **2008**, *20*, 6792–6797.
(13) Li, Y.; Lv, X.; Lu, J.; Li, J. *J. Phys. Chem. C.* **2010**, *114*, 21770–21774.
(14) Kamat, P. V. *J. Phys. Chem. Lett.* **2010**, *1*, 520–527.
(15) Muszynski, R.; Seger, B.; Kamat, P. V. *J. Phys. Chem. C.* **2008**, *112*, 5263–5266.
(16) Goncalves, G.; Marques, P. A. A. P.; Granadeiro, C. M.; Nogueira, H. I. S.; Singh, M. K.; Gracio, J. *Chem. Mater.* **2009**, *21*, 4796–4802.
(17) Padgett, C. W.; Brenner, B. W. *Nano Lett.* **2004**, *4*, 1051–1053.
(18) Kongkanand, A.; Vinodgopal, K.; Kuwabata, S.; Kamat, P. V. *J. Phys. Chem. B* **2006**, *110*, 16185–16188.
(19) Ostojic, G. N.; Ireland, J. R.; Hersam, M. C. *Langmuir* **2008**, *24*, 9784–9789.
(20) Bayati, M.; Abad, J. M.; Nichols, R. J.; Schiffrin, D. J. *J. Phys. Chem. C.* **2010**, *114*, 18439–18448.
(21) Ren, G.; Xing, Y. *Nanotechnology* **2006**, *17*, 5596–5601.
(22) Lin, Y.; Watson, K. A.; Fallbach, M. J.; Ghose, S.; Smith, J. G., Jr.; Delozier, D. M.; Cao, W.; Crooks, R. E.; Connell, J. W. *ACS Nano* **2009**, *3*, 871–884.
(23) Teranishi, T.; Miyake, M. *Chem. Mater.* **1998**, *10*, 594–600.
(24) Leff, D. V. *J. Phys. Chem.* **1995**, *99*, 7036–7041.
(25) Do. I. *Ph.D dissertation*, Michigan State University, East Lansing, MI, 2006.
(26) Meguro, K.; Torizuka, M.; Esumi, K. *Bull. Chem. Soc. Jpn.* **1988**, *61*, 341–345.
(27) Mohamed, M. B.; Wang, Z. L.; El-Sayed, M. A. *J. Phys. Chem. A.* **1999**, *103*, 10255–10259.
(28) Drzal, L. T.; Do, I. H.; Fukushima, H. *Method For Producing Compositions Of Nanoparticles On Solid Surfaces*. U.S. Patent Application 11/435 498, 2006.
(29) Jasuja, K.; Linn, J.; Melton, S.; Berry, V. *J. Phys. Chem. Lett.* **2010**, *1*, 1853–1860.
(30) Vinodgopal, K.; Neppolian, B.; Lightcap, I. V.; Grieser, F.; Ashokkumar, M.; Kamat, P. V. *J. Phys. Chem. Lett.* **2010**, *1*, 1987–1993.
(31) Drzal, L. T.; Fukushima, H. *Expanded Graphite And Products Produced Therefrom*. U.S. Patent Application 11/363 336, 2006.
(32) Fukushima, H.; . *Ph.D dissertation*, Michigan State University, East Lansing, MI, 2003.
(33) Hiemenz, P. C.; Rajagopalan, R. In *Principles of colloid and surface chemistry*. 3rd ed., revised and expanded; Marcel Dekker: New York; 1997, pp 575−614.
(34) Bai, L.; Zhu, H.; Thrasher, J. S.; Street, S. C. *ACS App. Mater. Interfaces* **2009**, *1*, 2304–2311.
(35) Kuo, P. L.; Chen, W. F.; Huang, H. Y.; Chang, I. C.; Dai, S. A. *J. Phys. Chem. B* **2006**, *110*, 3071–3077.
(36) Sun, X.; Dong, S.; Wang, E. *Polymer.* **2004**, *45*, 2181–2184.
(37) Zhang, J.; Xu, Q.; Ye, F.; Lin, Q.; Jiang, D.; Iwasa, M. *Colloids Surf., A.* **2006**, *276*, 168–175.
(38) Oxtoby, D. W. *Acc. Chem. Res.* **1998**, *31*, 91–97.
(39) Furedi-Millhofer, H. *Pure Appl. Chem.* **1981**, *53*, 2041–2055.
(40) Peng, X. G.; Wickham, J.; Alivisatos, A. P. *J. Am. Chem. Soc.* **1998**, *120*, 5343–5344.
(41) Xiang, J.; Drzal, L. T. *Carbon* **2011**, *49*, 773–778.
(42) Nan, C. W.; Liu, G.; Lin, Y.; Li, M. *Appl. Phys. Lett.* **2004**, *85*, 3549–3551.
(43) Huxtable, S.; Cahill, D. G.; Shenogin, S.; Xue, L.; Ozisik, R.; Barone, P.; Usrey, M.; Strano, M. S.; Siddons, G.; Shim, M.; Keblinski, P. *Nat. Mater.* **2003**, *2*, 731–734.
(44) Schmidt, A. J.; Chen, X.; Chen, G.; *Rev. Sci. Instrum.* **2008**, *79*, 114902(1−9).
(45) Wang, Z.; Xie, R.; Bui, C. T.; Liu, D.; Ni, X.; Li, B.; Thong, J. T. L. *Nano Lett.* **2011**, *11*, 113–118.
(46) Morgan, G. J.; Uher, C. *Philos. Mag., B* **1981**, *44*, 427–430.
(47) Luo, T.; Lloyd, J. R. *Int. J. Heat Mass Transfer* **2010**, *53*, 1–11.
(48) Kong, B. S.; Geng, J.; Jung, H. T. *Chem. Commun.* **2009**, *16*, 2174–2176.
(49) Shi, Y.; Kim, K. K.; Reina, A.; Hofmann, M.; Li, L. J.; Kong, J. *ACS Nano* **2010**, *4*, 2689–2694.
(50) Kim, K. K.; Reina, A.; Shi, Y.; Park, H.; Li, L. J.; Lee, Y. H.; Kong, J.; *Nanotechnology*, **2010**, *21*, 285205(1−6).